Proceedings of the INMM & ESARDA Joint Virtual Annual Meeting
August 23-26 & August 30-September 1, 2021

Aspects of Crystal Growth and Atomic-Scale Characterization of U/Th Age-Dating Particles

Katherine Koh
Pacific Northwest National Laboratory

Riane Stene
Pacific Northwest National Laboratory

Stephan Vogt
Pacific Northwest National Laboratory

Tim Pope
Pacific Northwest National Laboratory

Alan Albrecht
Pacific Northwest National Laboratory

Chris Barrett
Pacific Northwest National Laboratory

ABSTRACT

Trace analysis of particulate material collected on environmental swipe samples continues to be one of the cornerstones of the IAEA's process of verifying member state compliance as part of the Non-Proliferation Treaty (NPT).[1, 2] While complementary to traditional bulk analysis, the ability to measure individual particles can be far more impactful from a radiochronometry perspective. In radiochronometry, the "age" of the material ideally records the time when the material was last chemically separated and purified. Capturing this information from individual particles provides a much more detailed record of a nuclear facility's operational history. Consequently, the $^{234}U/^{230}Th$ radiochronometer is being evaluated as a means of establishing model ages for discrete particles with sufficient confidence.[3] To support the extension of current capabilities, reference materials with a suitable particle form factor and well-documented purification date are actively sought for development with large geometry secondary ion mass spectroscopy (LG-SIMS).

To meet this need, PNNL is formulating a range of fit-for-purpose uranium particles standards that address the changing criteria encountered with the incremental development of an LG-SIMS age-dating methodology. PNNL's current inventory of UO_2 particle standards has been designed and tailored for interlaboratory comparisons between the IAEA Environmental Sample Laboratory (IAEA-ESL) and the expansive Network of Analytical Laboratories (NWAL). Building on this initial foundation, a modified chemical strategy for the hydrothermal synthesis and growth of single-crystal $Th_{1-x}U_xO_2$ particles is being explored. In this work, considerations surrounding initial chemical separation, precursor formulation, and finely controlled synthesis of homogeneous particles will be outlined. Mechanistic details of PNNL's particle synthesis strategy and the thorough characterization of elemental composition, crystal structure, and isotopic profile will be discussed at length.

INTRODUCTION

Characterization of chemical and physical properties of nuclear materials is an essential instrument in nuclear safeguards verification activities.[2] Typical properties investigated, such as the uranium and plutonium isotopic composition, uranium/plutonium elemental ratios, trace elemental contents, and more, can provide the materials' nuclear pedigree and assist in verifying safeguards declarations.[4, 5] The isotopic analysis of individual particles, as collected on environmental swipe samples by IAEA inspectors, is a powerful method that has become standard for IAEA verification efforts to verify the correctness and completeness of nuclear material declarations from a facility. Additionally, the $^{230}Th/^{234}U$ ratio measured in environmental samples can be used to determine the "age" of the sample (i.e., the date since the sample's last purification).[3]

Modern, state-of-the-art analytical techniques such as Large Geometry-Secondary Ion Mass Spectrometry (LG-SIMS) or Thermal Ionization Mass Spectrometry (TIMS) can detect extremely small amounts of these radionuclides in individual particles.[6-8] For highly accurate and precise measurements, reference and quality control materials are needed with well-characterized $^{230}Th/^{234}U$ ratios.

Leveraging its current capability to produce uranium particle reference material, PNNL has been working on developing unique isotopic formulations and particle synthesis techniques that will afford a supply of fit-for-purpose reference materials for $^{230}Th/^{234}U$ age-dating. Herein, recent progress towards this goal using traditional hydrothermal synthesis and a newer microwave-assisted hydrothermal synthesis approach is introduced. Isotopic formulation of appropriate feedstocks for particle synthesis is outlined and discussed with respect to particle size and detection thresholds. Analytical techniques and the characterization data produced to inform the U/Th homogeneity of individual and bulk particles are introduced.

RESULTS & DISCUSSION

$^{234}U/^{230}Th$ Age-Dating Particles

As highlighted by Szakal et al. in their report on recent advancements in age-dating of individual particles, predicted confidence limits for measurements of material recently purified offer excellent utility for individual particle analysis given that the ^{234}U counts are an inverse scaling factor for $^{234}U/^{230}Th$ age-dating.[3] However, most of the certified reference material (CRM) currently available is 15 years or more beyond their purification date. While certainly useful in many respects, a more stable oxide chemical form is sought for LG-SIMS analysis. To this end, age-dating particle reference material ranging from 0-15 years was set as an initial target of this study.

Figure 1. Predicted concentrations of ^{230}Th for various CRMs with respect to particle size.

Uranium oxide particles, both doped with low concentrations of ^{230}Th (aged) and recently purified (fresh), were chosen as near-term needs in standing up a SIMS-based, age-dating capability. The method of reference material production outlined herein was designed to have the flexibility in producing particles with a size range of 1-5 µm (**Figure 1**). For the purposes of instrument calibration and benchmarking, larger particles offer more material for measurement and are longer lived under direct micro-beam analysis, with measurement proficiency tested with decreasing particle size.

Particle Synthesis & Size Control

A hydrothermal route for the phase-controlled synthesis of crystalline UO_2 particles was developed and tailored to meet the desired characteristics needed for milligram batches of reference material.[9] Hydrothermal synthesis is a well-established method of synthesizing colloid particles using a combination of high temperature and pressure. In this way, reaction mechanisms not achievable at standard temperature and pressure can be performed within the confinement of a Teflon-lined, stainless steel pressure vessel. The specific method described herein uses organic amines as both reducing agents and structure-directing ligands, further simplifying the synthetic procedure. In its acetate form, uranyl ions are found to readily complex with ethylenediamine, which then undergoes a thermolysis reaction that triggers the nucleation and growth of UO_2 crystals.

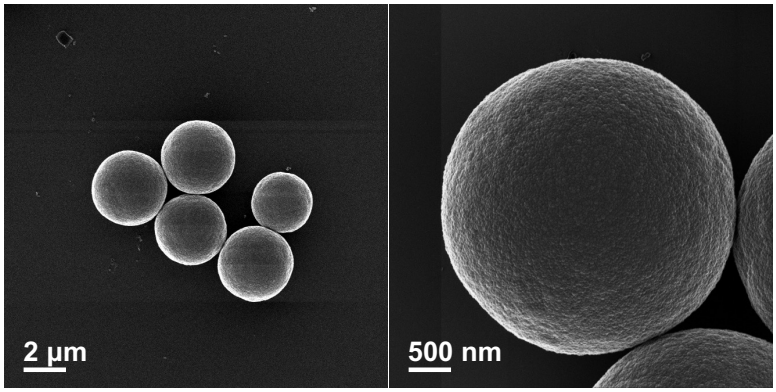

Figure 2. Larger-sized UO_2 particles prepared with depleted material.

Using a combination of increased precursor concentration and longer synthesis times, the previous hydrothermal synthesis protocol was successfully tailored to produce larger (2-3 µm) UO_2 particles (**Figure 2**). The particles were prepared from depleted uranium material and display a spherical morphology. The synthesis of larger-sized particles is primarily dependent on precursor concentration and reaction time. Compared to the method reported previously, this synthesis process requires 10x as much uranyl acetate and a full week of reaction time at 160°C.

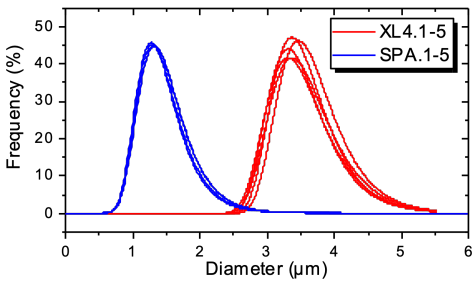

XL4.1-5	
Median size	3.22 (µm)
Mean size	3.26 (µm)
Variance	1.36E^{-1} (µm^2)
St. Dev.	0.37 (µm)
Mode size	3.20 (µm)
Geo. mean size	3.24 (µm)
Geo. variance	1.01 (µm^2)

Figure 3. Particle size analysis collected from suspensions of UO_2 particles from a two-day reaction (blue) and seven-day reaction (red), with a corresponding summary of measured values for XL4.1-5.

Figure 3 shows a typical size distribution for particles synthesized with two days of hydrothermal growth (SPA.1-5) and particles collected from a seven-day reaction (XL4.1-5). As is clearly evident, particles prepared with lower concentrations of uranyl acetate precursor (20 mg) and short growth times (48 hours) display an average diameter centered around 1-1.2 µm in size. Extending growth time out to 7 days and increasing the concentration of uranium monomer in the reaction to 250 mg generates UO_2 particles of much larger sizes (~3.3 µm). Based on the results

of this analysis, the new synthesis protocol produces an optimum size distribution for U/Th age dating. At an average diameter of 3.26 μm, sufficient concentrations of ^{230}Th should be present within individual particles down to enriched levels of ^{235}U of 10%. Smaller particle sizes would likely necessitate much higher levels of enrichment for ages less than 15 years.

Controlled Thorium Doping of UO_2 Particles

To evaluate the Th doping behavior in the UO_2 particle synthesis method, several batches of particles were prepared with varying concentrations of Th nitrate stock solution. Th-doped particles were produced according to the larger particle synthesis protocol discussed previously, with variations made to the added DI water to accommodate the addition of a Th spike. This ensured that the total volume of the reaction solution remained constant and that identical pressure conditions were generated during heating. A 10 mg/L stock solution of natural Th nitrate was used in the doping process. Synthesized particles were extracted and cleaned using standard centrifuge precipitation, which entails multiple washing and sonication steps with DI water, IPA, and Vertrel. Effective washing and removal of all unreacted U and Th precursor was critically important to the doping evaluation as only solid incorporated Th was being studied.

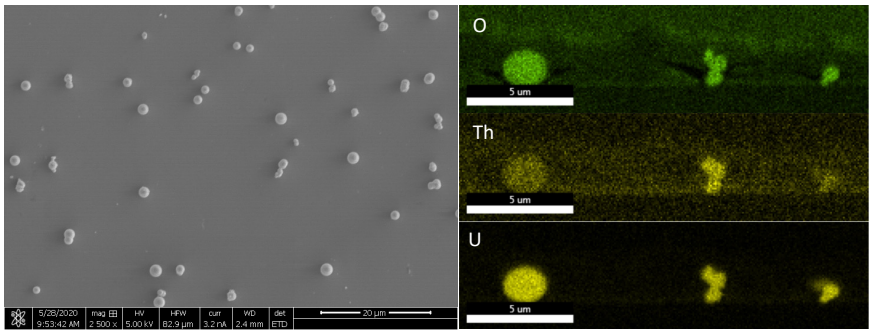

Figure 4. SEM image of Th-doped UO_2 particles with corresponding EDS elemental maps.

Inspection of particle size and morphology from batches of Th-doped UO_2 found no discernable differences from undoped UO_2 particles and no evidence of a secondary crystalline or amorphous phase. The similar fluorite crystal structures of UO_2 and ThO_2 allow both materials to co-crystallize during hydrothermal synthesis. **Figure 4** shows a top-down SEM of Th-doped (10 mg/L) UO_2 particles dispersed across a silicon substrate. A focused ion beam (FIB) was used to isolate three individual particles by selectively depositing platinum and then slicing through the particles with gallium ions. Cross-sectioned particles were found to have pore fractions of 5-15%, a number similar for undoped UO_2 particles. This observation tracks with the same trend identified in earlier work with older uranyl acetate precursors, where polycrystalline particles were formed. EDS analysis taken from the same cross-sectioned region showed strong evidence that Th is incorporated into the UO_2 particles in a co-crystallization process. It would also seem that the Th is homogeneously distributed within the particles, with no evidence of pure ThO_2 particles or UO_2 and ThO_2 agglomerates observed.

Aliquots of each batch of particles were dissolved in concentrated nitric acid and then diluted to a nitric acid concentration of 2%. To benchmark the room temperature acid dissolution, two duplicate samples (XL3-HT and XL4-HT) were prepared in nitric acid and then heated in an acid digestion autoclave. The results of the ICP-MS analysis of total U and ^{232}Th from each batch of particles are shown in **Table 1**.

Table 1. Bulk ICP-MS analysis from a series of Th doped and undoped UO_2 synthesis reactions.

Sample ID	Log-in #	U-total		^{232}Th		$Th(NO_3)_4$ Spike	Th/U
		ng analyte/g sample solution as rec'd ± 1s				ppm	ratio
blank 2%HNO_3	20-0022-1	0.204	0.001	0.0043	0.0001	0	0.0213
XL3	20-0022-2	4043	13	0.0282	0.0003	0	0.0000
XL4	20-0022-3	5392	22	145	0.4	10	0.0269
XL5	20-0022-4	6074	17	170	0.8	10	0.0280
XL6	20-0022-5	5408	4	1333	18.2	100	0.2466
XL13	20-0022-8	4171	11	9832	1.7	1000	2.3572
XL14	20-0022-9	4663	3	13	7.2	0.1	0.0027
XL3-HT	20-0022-6	3808	17	0.032	0.001	0	0.0000
XL4-HT	20-0022-7	5671	25	147	1	10	0.0259

The nitric acid blank was found to contain trace levels of U and Th ions. Particles from XL3, which did not receive a Th nitrate spike, were also found to have trace amounts of Th. As can be seen from XL3/XL4 and XL3-HT/XL4-HT, no measurable differences were noted for room temperature acid dissolution and the high temperature and pressure acid digestion techniques. This comparison also shows that acid heating is not needed to ensure the full dissolution of the particles. It was initially feared that some U and Th might be lost to the Teflon beakers due to sorption at higher temperatures, but that phenomenon was not observed to any measurable degree. For particles spiked with varying concentrations of Th, a clear, linear trend can be seen between the amount of Th added and the concentration of Th measured in the resulting particles. However, batch-to-batch variations may require further study as the difference in the U/Th ratio in XL4 and XL5 is statistically significant when considering the age-dating application for these particles. That said, this data provides a workable correction factor for future U/Th particle production activities.

The maps shown in **Figure 5** were collected for the three main constituents identified in the lamella, i.e., U, O, and Pt. Note that Pt was used as a stabilizing capping layer during FIB sample preparation. The particle was found to be uniformly uranium oxide, with no trace of Th detected.

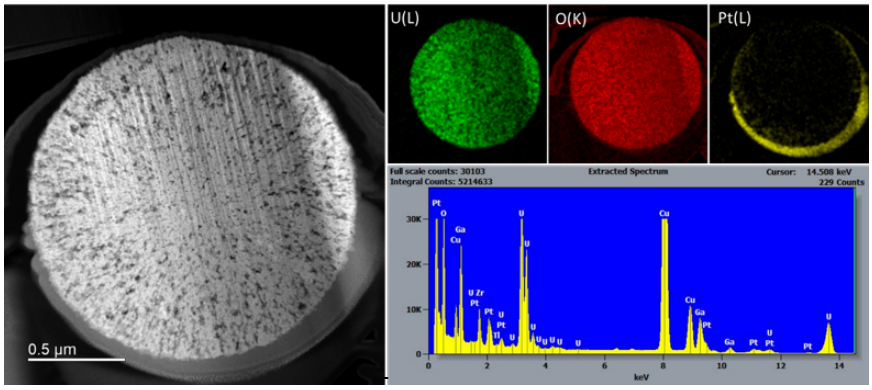

Figure 5. HAADF image, EDS maps, and corresponding spectrum collected on a FIB lamella extracted from a UO_2 particle prepared using the larger particle synthesis protocol (No Thorium).

Elemental mapping from regions of the $U_XTh_{1-X}O_2$ lamella (**Figure 6**) identified strong signals from U, O, and slightly weaker signals from Th. That said, the elemental ratio of U:Th:O was found to be uniform across the sample and consistent with previous measurements made by SEM/EDS. EDS spectrum in Figure 6 shows distinct peak positions for Th Lα (12.967) and M (2.991) edges.

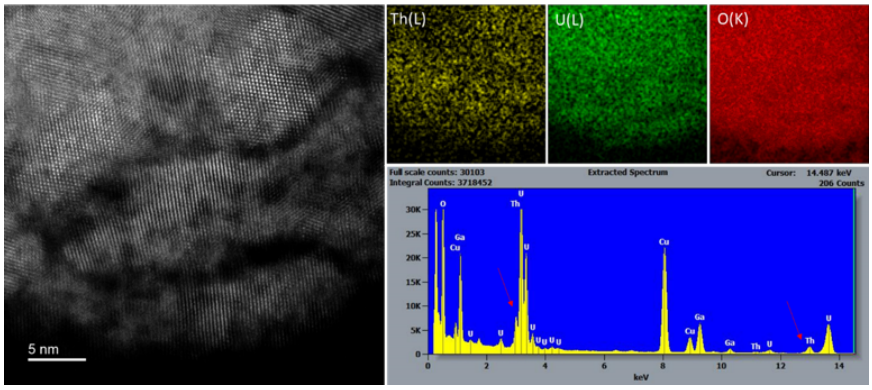

Figure 6. HAADF image, EDS maps, and corresponding spectrum collected on a FIB lamella extracted from a $U_XTh_{1-X}O_2$ particle prepared using thorium nitrate doping together with uranium synthesis protocol (Thorium Doped).

Microwave-Assisted Hydrothermal Synthesis

In past PNNL production cycles of uranium particle reference materials for the IAEA Environmental Sample Laboratory, the chemical purity of the uranium precursor was found to dramatically change the resulting particle crystallinity and morphology. Instead of forming spherical polycrystalline UO_2 particles, octahedral-shaped, single-crystal UO_2 particles were grown with identical reaction conditions. It was later discovered that the uranium acetate precursor, which was formulated from several different CRMs, had gone through a number of chemical transformations (metal, oxide, nitrate, oxide, acetate) and was eventually re-crystallized as uranyl acetate dihydrate. The removal of impurities, such as uranium carbonate, resulted in the growth of octahedral-shaped particles, as shown in **Figure 7**. In qualification and proficiency testing with LG-SIMS, the uniformly dense single-crystal UO_2 particles showed much longer-lived signal intensities when compared to polycrystalline UO_2 particles. To this end, a more purposeful strategy for the synthesis of single-crystal particles is being explored for $^{234}U/^{230}Th$ age-dating reference material using a technique referred to as microwave-assisted hydrothermal synthesis.

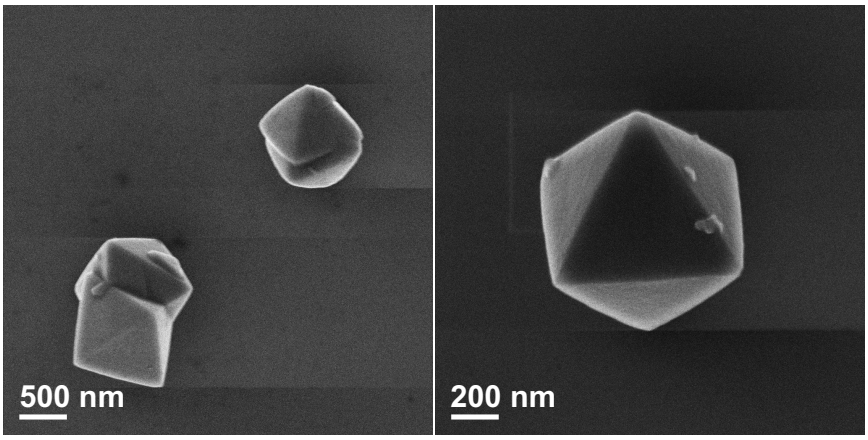

Figure 7. Helium ion images of octahedral-shaped, single-crystal UO_2 particles.

Traditional hydrothermal synthesis is typically performed in a Teflon-lined, stainless-steel autoclave.[10] To reach appropriate growth temperatures, the vessel is heated through convection in an oven or furnace, slowly ramping to a desired setpoint for crystal growth. As the term implies,

microwave-assisted hydrothermal synthesis uses specific microwave frequencies to heat the reaction solution directly and rapidly in an autoclave. The resulting temperature ramp profile is much steeper, with greater control of setpoints afford with internal infrared sensors. To test these augmented capabilities, a series of cerium oxide syntheses were conducted. As many other reports have documented, CeO_2 is the preferred non-radioactive analog for uranium oxide, which crystallizes with the same fluorite crystal structure.[11]

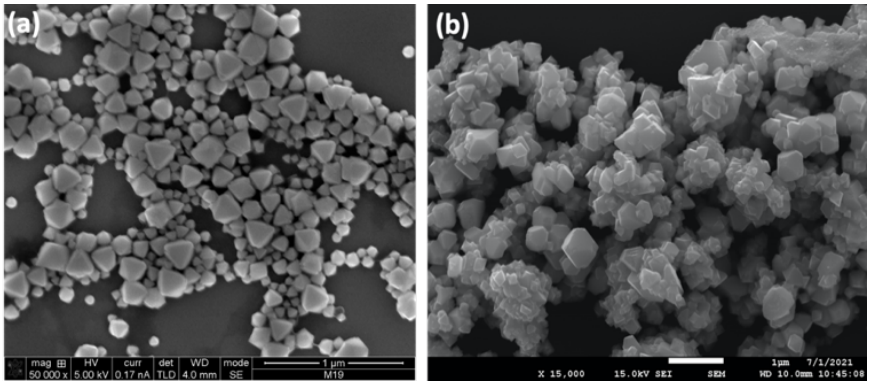

Figure 8. SEM images of CeO_2 (a) with PVP (4:1 molar ratio of PVP:Ce) and (b) without PVP.

In a typical procedure, $Ce(NO_3)_3 \cdot 6H_2O$ (0.0753 g) and PVP (0.0378 g) were dissolved in a mixed solvent of anhydrous ethanol (1.5 mL) and deionized water (15.3 mL) in 100 mL Teflon vessels. The mixed solution was ultrasonically agitated for 5 min at room temperature and then transferred into a high-pressure vessel, sealed, and was subjected to microwave treatment at 180°C for 30 min, with a power of 6 W using an Anton Parr Microwave Go. After cooling, the precipitated material obtained from the reaction vessel was collected and washed with deionized water and absolute ethanol several times. Residual PVP surfactant was removed with successive washing steps with Vertrel.

The majority of the resulting CeO_2 particles were found to have a distinct octahedral-shaped morphology, as can be seen in **Figure 8(a)**. As previously seen with single-crystal UO_2 particles, the isotropic crystal growth of compounds with a fluorite lattice structure generally develops into an octahedron, enclosed by eight (111) facets. An SEM survey of particle size found a range of 50-200, with larger particles having a much more apparent octahedral shape. Unlike the previous hydrothermal method, this synthesis protocol utilizes a surfactant as a structure-directing ligand. Removal of the surfactant from the reaction results in the formation of larger, micron-sized particles, shown in **Figure 8(b)**. However, without a surfactant, crystalline agglomerates, several microns in size, form a large fraction of the sample.

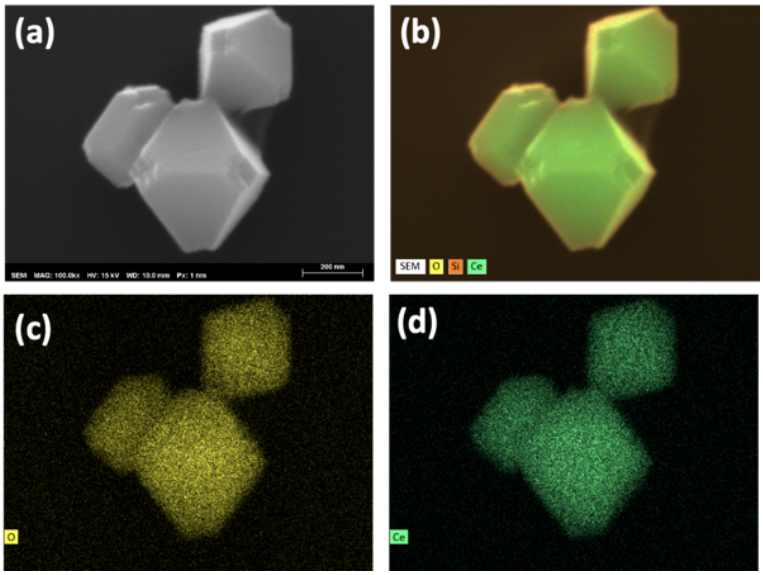

Figure 9. SEM and corresponding EDS mapping of CeO_2 particles after 6 hrs of microwave treatment at 180 °C. (a) the original SEM image of CeO_2, (b) combined elemental analysis result from Si and O and Ce, (c) elemental map of oxygen, and (d) Ce.

Higher magnification SEM imaging identified residual PVP surfactant adhered to CeO_2 particles despite numerous washing treatments (**Figure 9(a)**). Calcination of particle material in air at 400 °C was found to remove any remaining organic material. EDS mapping, highlighted in **Figures 9(c)** and **9(d)**, confirmed the singular chemical composition of cerium oxide, with no other detectable impurities.

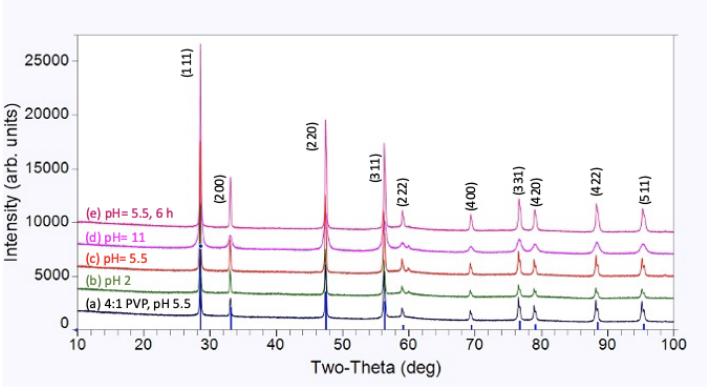

Figure 10. XRD of (a) 4:1 ratio of PVP to Ce without pH adjustments, (b) without surfactant but pH adjusted to 2 by adding HNO_3, (c) without surfactant, without pH adjustments, (d) without surfactant but pH 11 by adding NaOH, and (e) longer reaction time of 6 hrs. The reference (blue line) material is cerianite $Ce•CeO_2$.

The crystallinity of as-synthesized CeO_2 particles (pH 5.5) and several other batches of particles synthesized without PVP surfactant and/or adjusted solution pH was determined by XRD analysis. The strong and sharp diffraction peaks in **Figure 10** indicate highly crystalline material in all samples. The XRD pattern can be indexed to pure face-centered cubic (fcc) fluorite CeO_2 with a lattice constant of a = 5.41 Å (JCPDS card no. 34-0394). No additional peaks or changes in peak width were observed by XRD for pH-adjusted conditions.

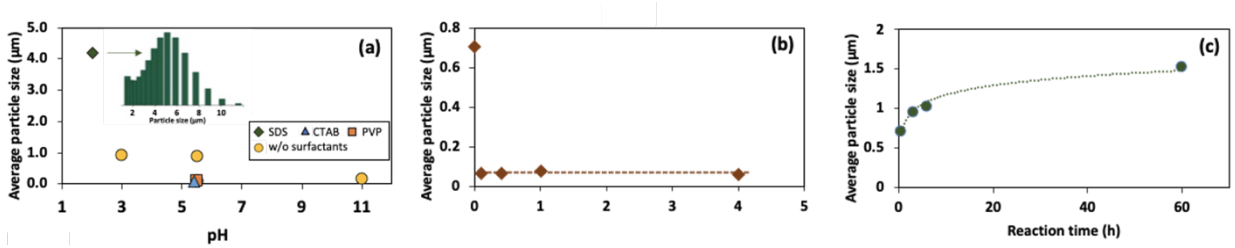

Figure 11. Average CeO_2 particle sizes vs. (a) pH after 30 min of microwave treatment (180 °C), (b) amount of PVP, (c) reaction time. Average particle sizes were measured by laser diffractometry, and all reactions were performed with microwave heating at 180 °C. Inset graph in (a) shows particle size distribution.

With the addition of PVP surfactant dictating the resulting particle size of as-synthesized CeO_2 particles, a series of alterations were made to the reaction conditions in an effort to control particle size. Four main factors were investigated, specifically solution pH, surfactant concentration, reaction time, and surfactant type. In the case of the latter variable, the addition of SDS and CTAB disrupted the formation of octahedral-shaped particles, resulting in large agglomerates in the case of SDS, and nanoparticles when using CTAB. Bulk particle size analysis (**Figure 11(a)**) collected by laser diffractometry measured an average particle size for SDS and CTAB ceria particles at ~5 μm and 20 nm, respectively. Impact due to reaction pH was also studied, with an increase of average particle size ~1 μm noted at pH 3 and 5.5, and no measurable size change at pH 11. To remove contributions due to surfactant, PVP was omitted in all cases. Changes to the molar ratio of PVP/Ce, outlined in **Figure 11(b)**, resulted in little to no change in particle size with increasing PVP concentrations. However, as previously noted, the complete removal of PVP increased the average diameter to ~700 nm. **Figure 11(c)** shows the change in ceria particle size as a function of reaction time. As can be seen, particle size is quickly defined in the first few hours of the reaction, with extending heating times out to 60 hours only increasing the average particle size to 1.5 μm.

CONCLUSIONS

Hydrothermal synthesis of uranium oxide particles has been shown to be a reliable approach to the generation of suitable reference material in support of nuclear safeguards activities with LG-SIMS analysis. The extension of this chemical pathway to $^{230}Th/^{234}U$ age-dating particles is currently focused on the generation of larger particles (1-5 μm) with sufficient concentrations of both isotopes for optimum measurement statistics. The modified approach reported here is tailored to particles with an average diameter of 3.26 μm, which our calculations show as sufficient for age-dating on several natural, low, and high enriched CRMs. We also show that the synthesis method can be spiked with thorium nitrate to generate artificially high concentrations of Th in UO_2 particles. Th distribution was found to be uniformly incorporated within UO_2 particles owing to a co-crystallization process driven by the similar fluorite lattice structure of thoria and uraninite. Finally, a new synthetic approach was evaluated with the synthesis of single-crystal CeO_2 particles. The use of microwave-assisted hydrothermal synthesis offers a number of synthetic advantages that need to be explored further. Further, the use of a nitrate precursor compound in place of acetate precursor appears to reliably form single-crystal particles as opposed to polycrystalline variants. Future efforts will be focused on the extension of this new technique to $Ce_{1-x}U_xO_2$ and $Th_{1-x}U_xO_2$.

ACKNOWLEDGMENTS

The authors wish to thank the team at the IAEA Environmental Sample Laboratory for their expert advice and critical feedback throughout this work. The Pacific Northwest National Laboratory is operated for the U.S. Department of Energy by Battelle Memorial Institute under Contract No. DE-AC05-76RL01830. This work was sponsored by the U.S. Department of Energy, National Nuclear Security Administration, Office of International Nuclear Safeguards.

REFERENCES

1. Cooley, J. *Environmental Sampling*; International Atomic Energy Agency: 1998.
2. Donohue, D. L., Strengthening IAEA safeguards through environmental sampling and analysis. *Journal of Alloys and Compounds* **1998,** *271-273*, 11-18.
3. Szakal, C.; Simons, D. S.; Fassett, J. D.; Fahey, A. J., Advances in age-dating of individual uranium particles by large geometry secondary ion mass spectrometry. *Analyst* **2019,** *144* (14), 4219-4232.
4. Lantzos, I.; Kouvalaki, C.; Nicolaou, G., Plutonium fingerprinting in nuclear forensics of spent nuclear fuel. *Progress in Nuclear Energy* **2015,** *85*, 333-336.
5. Mayer, K.; Wallenius, M.; Varga, Z., Nuclear Forensic Science: Correlating Measurable Material Parameters to the History of Nuclear Material. *Chemical Reviews* **2013,** *113* (2), 884-900.
6. Fauré, A.-L.; Dalger, T., Age Dating of Individual Micrometer-Sized Uranium Particles by Secondary Ion Mass Spectrometry: An Additional Fingerprint for Nuclear Safeguards Purposes. *Analytical Chemistry* **2017,** *89* (12), 6663-6669.
7. Hedberg, P. M. L.; Peres, P.; Fernandes, F.; Renaud, L., Multiple ion counting measurement strategies by SIMS – a case study from nuclear safeguards and forensics. *Journal of Analytical Atomic Spectrometry* **2015,** *30* (12), 2516-2524.
8. Ranebo, Y.; Hedberg, P. M. L.; Whitehouse, M. J.; Ingeneri, K.; Littmann, S., Improved isotopic SIMS measurements of uranium particles for nuclear safeguard purposes. *Journal of Analytical Atomic Spectrometry* **2009,** *24* (3).
9. Belai, N.; Frisch, M.; Ilton, E. S.; Ravel, B.; Cahill, C. L., Pentavalent Uranium Oxide via Reduction of $[UO2]^{2+}$ Under Hydrothermal Reaction Conditions†. *Inorganic Chemistry* **2008,** *47* (21), 10135-10140.
10. Shi, J.; Wang, H.; Liu, Y.; Ren, X.; Sun, H.; Lv, B., Rapid microwave-assisted hydrothermal synthesis of CeO2 octahedra with mixed valence states and their catalytic activity for thermal decomposition of ammonium perchlorate. *Inorganic Chemistry Frontiers* **2019,** *6* (7), 1735-1743.
11. Stennett, M. C.; Corkhill, C. L.; Marshall, L. A.; Hyatt, N. C., Preparation, characterisation and dissolution of a CeO2 analogue for UO2 nuclear fuel. *Journal of Nuclear Materials* **2013,** *432* (1), 182-188.